

REPORT DOCUMENTATION PAGE

Form Approved
OMB No. 0704-0188

2

AD-A243 055



estimated to average 1 hour per response, including the time for reviewing instructions, searching existing data sources, gathering and reviewing the collection of information. Send comments regarding this burden estimate or any other aspect of this reporting burden, to Washington Headquarters Services, Directorate for Information Operations and Reports, 1215 Jefferson Avenue, Washington, DC 20540, and to the Office of Management and Budget, Paperwork Reduction Project (0704-0188), Washington, DC 20503.

REPORT DATE: 3. REPORT TYPE AND DATES COVERED: FINAL 15 Apr 88 TO 14 Oct 91

4. TITLE AND SUBTITLE: III-V Modulation and Switching devices for Optical system applications
5. FUNDING NUMBERS: 2305/B4

6. AUTHOR(S): Professor Singh

7. PERFORMING ORGANIZATION NAME(S) AND ADDRESS(ES): University of Michigan, Dept of Electrical Engineering & Computer Science, Ann Arbor, MI 48109-2122
AFOSR-TR-91 0927

8. PERFORMING ORGANIZATION REPORT NUMBER

9. SPONSORING / MONITORING AGENCY NAME(S) AND ADDRESS(ES): AFOSR/NE, Bldg 410, Bolling AFB Washington DC 20332-6448, Dr. Alan E. Craig

10. SPONSORING / MONITORING AGENCY REPORT NUMBER: AFOSR-88-0168

11. SUPPLEMENTARY NOTES: DTIC ELECTRA 88-0168

12a. DISTRIBUTION / AVAILABILITY STATEMENT: APPROVED FOR PUBLIC RELEASE: DISTRIBUTION IS UNLIMITED

12b. DISTRIBUTION CODE

13. ABSTRACT (Maximum 200 words)
Optical computing has been a blue sky dream for scientists for over a decade. In several areas optical processing has made great strides (1-4). These areas include optical communication, optical memory, optical scanning, etc. However the "optical computer" still remains a dream. Earlier spectacular successes in very high speed optical switches based upon non-linear optical effects in III-V compound semiconductor structures have not led to useful applications. Even in optical communication, the full potential of optics remains unrealized because of lack of more tailorable devices such as wavelength selective detectors.

14. SUBJECT TERMS: 91-16544

15. NUMBER OF PAGES
16. PRICE CODE

17. SECURITY CLASSIFICATION OF REPORT: UNCLASSIFIED

18. SECURITY CLASSIFICATION OF THIS PAGE: UNCLASSIFIED

19. SECURITY CLASSIFICATION OF ABSTRACT: UNCLASSIFIED

20. LIMITATION OF ABSTRACT: UNLIMITED

sm

**FINAL TECHNICAL REPORT: III-V
MODULATION AND SWITCHING DEVICES
FOR OPTICAL SYSTEMS APPLICATIONS**

Principal Investigator:
Professor Jasprit Singh

Co-Principal Investigator:
Professor Pallab Bhattacharya

Department of Electrical Engineering and Computer
Science The University of Michigan, Ann Arbor, MI
48109-2122

Submitted to

Air Force Office of Scientific Research
Bolling Air Force Base

Accession for	
NS	
DTIC TAB	
Unannounced	
Justification	
By	
Organization	
Availability	See
Availability	See
120	See 1
A-1	



1. BACKGROUND:

Optical computing has been a blue sky dream for scientists for over a decade. In several areas optical processing has made great strides⁽¹⁻⁴⁾. These areas include optical communication, optical memory, optical scanning, etc. However the "optical computer" still remains a dream. Earlier spectacular successes in very high speed optical switches based upon non-linear optical effects in III-V compound semiconductor structures have not led to useful applications. Even in optical communication, the full potential of optics remains unrealized because of lack of more tailorable devices such as wavelength selective detectors.

As one takes stock of the last decade or so of progress in optical computing, several important outcomes emerge. It appears clear that for maximized impact, optics must combine with electronics. Opto-electronic devices rather than all optical devices are more likely to impact important applications. It is also clear that to capture the power of optics, novel highly tailored devices are needed. To avoid the trap into which much of the earlier work on high optical intensity non-linear logic devices fell, the new devices must be tested for their application to in real opto-electronic systems. One area which holds exceptional promise in this regard is the quantum confined Stark effect (QCSE)⁽⁵⁻⁸⁾. This effect allows one to tailor the device response to such a great extent that at least in principle, a number of powerful devices can be conceived and demonstrated.

The first demonstration of active logic devices based on QCSE was the self-electro-optic-effect-device (SEED), where the optical (or electronic) state of the device could be altered by light intensity⁽⁸⁾. A variation on the SEED device was introduced by including an external transistor to amplify the photocurrent, so as to allow electronic gain on the device⁽⁹⁾. This allowed the use of low optical power consistent with semiconductor laser diode technology. High gain was ($\sim 20 - 100$) obtained at the University of Michigan by integrating a multiquantum well (MQW) structure into the base collector region of an HBT^(10,11), thus producing a versatile device compatible with HBT technology, the p-i-n modulator, p-i-n detector and laser technology. We will discuss some of the features of this device technology applicable in special and general purpose computing.

Excitonic transitions arise from electron-hole states coupled via the Columbic interaction. In presence of an electric field, the excitons dissociate at small electronic fields (≤ 10 kV/cm) in bulk semiconductors, but in quantum wells where the exciton is confined by strong barriers, the exciton position shifts to lower energies with applied bias without significant loss in the absorption peak. This effect, known as QCSE^(5,8), can be exploited to produce an assortment of important characteristics illustrated schematically in Fig. 1.

In Fig. 1(a) we illustrate the source of the QCSE i.e. the movement of the electron and hole wavefunction to the opposite sides of the well in presence of the electric field and the reduction of the ground state electron and hole subband energies. Figure 1(b) shows the commonly used p-i(MQW)-n structure for applying the reverse bias for QCSE. The absorption coefficient displays the features shown in Fig. 1(c) where the two peaks correspond to the heavy hole (HH) and light hole (LH) transitions. When an electric field is applied, the spectra moves towards lower energy and this feature cannot

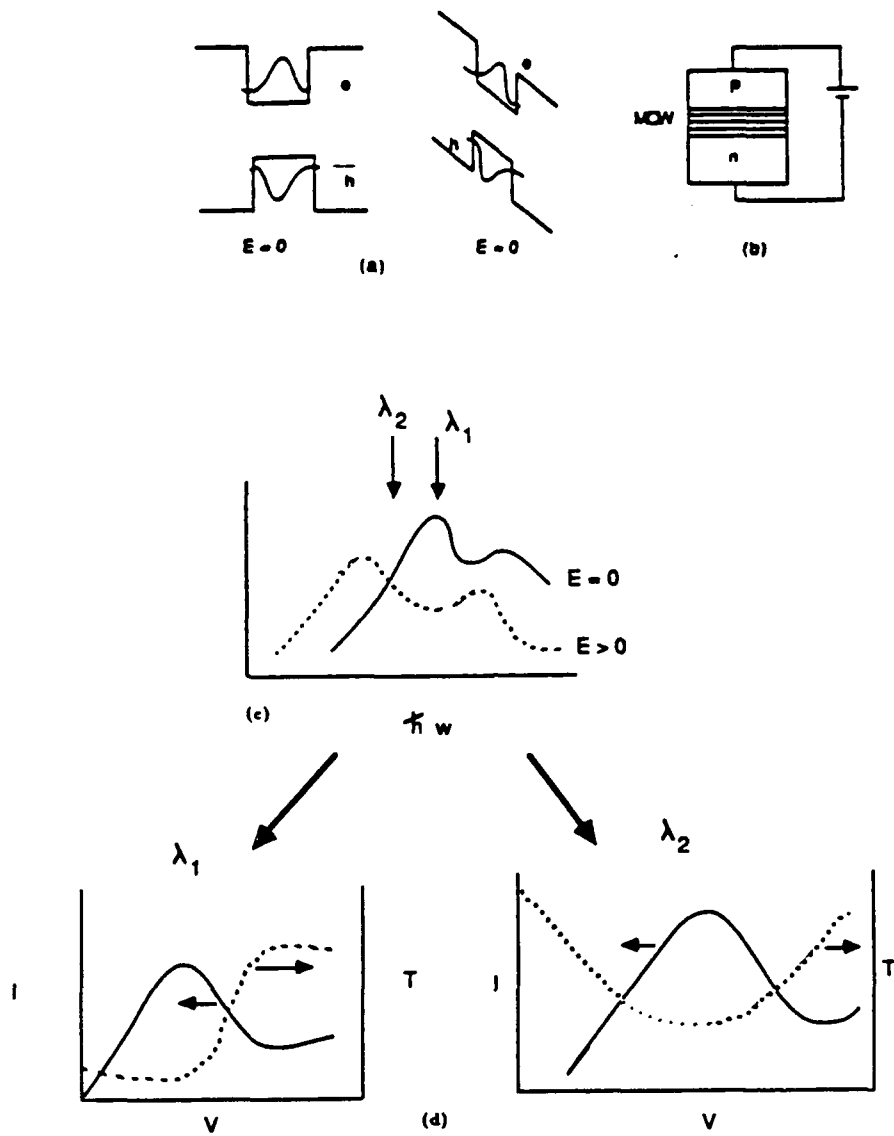


Figure 1: (a) A schematic of the electron and hole wavefunctions in absence and presence of an electric field in a quantum well; (b) a p-i(MQW)-n modulator; (c) excitonic absorption spectra in absence and presence of a field; (d) current-voltage and transmittance-voltage curves at different wavelengths.

only be exploited for optical modulation, but also has a very interesting effect on the photocurrent. At room temperature, the photocurrent is essentially proportional to the photons generated, even at fairly low applied bias⁽¹²⁾. The photocurrent versus applied bias curves can thus be tailored quite efficiently as shown in figure 1(d) where we show the photocurrent and transmittance through the structure at two different wavelengths λ_1 and λ_2 whose position is indicated in Fig. 1(c). As can be clearly seen, very different forms of I-V curves result. These curves can be exploited in ways which will be described next.

1.1 The MQW-HBT Controller-Modulator:

The potential of the negative resistance region of the I-V characteristics in a p-i(MQW)-n structure was realized by Miller et al⁽⁸⁾ and used to develop the SEED. Using a resistor in series with the p-i-n diode, the device can be shown to have efficient switching behavior as shown in Fig. 2. When the light intensity changes from I_2 to I_1 , the voltage across the device shifts from V_1 to V_2 causing a transmittance change from T_1 to T_2 . This basic device has spawned a number of other devices and has been the inspiration for the devices discussed below.

In order to make the SEED more compatible with the optical posers available in OEIC technology, it is important to have built-in electronic gain in the device. Gain is also essential for larger tolerance in the devices as well large fan-out and cascadability. Such gain can be realized by using an HBT with a MQW region in the base collector region. This device provides the following advantages:

- i) Since the HBT is a vertical device, a larger uniform potential can be developed across the base collector region to cause QCSE.
- ii) The third terminal i.e. the base allows one to efficiently coupled optical and electronic features.
- iii) The entire structure of the n^+ -p-i(MQW)-n HBT and the p-i(MQW)-n modulator can be grown epitaxially in one step. It is conceivable that the p-i-n structure could also form a laser which would be grown in the same planar growth. The structure is therefore very compatible with OEIC applications.

A schematic of the integrated MQW-HBT is shown in Fig. 3(a) along with the equivalent circuit. The MQW-HBT is shown in a circuit where it is controlling a modulator. The important point to realize is the presence of amplification of the photocurrent which allows low optical power switching. In a usual SEED the load resistances required are $\sim 100K\Omega$ with an applied bias of 10-15 volts. The load resistances and $\leq 5 K\Omega$ for the MQW-HBT's. An important asset of the MQW-HBT is that the I-V curves can be shifted either by optical power or through base current and as long as some optical power is present, the negative resistive region is maintained. In Fig. 3 we have shown schematically how the switching operation can be carried out using as input either the base current or the optical intensity. Also shown are potential applications.

The heterostructure for the controller-modulator is grown by us using MBE. The important features of the heterostructure are the following: first, the $0.4 \mu\text{m}$ thick $\text{Al}_{0.3}\text{Ga}_{0.7}\text{As}$ layer serves as an etch stop layer for selective substrate removal under the modulator. The collector region has the $0.6 \mu\text{m}$ undoped $\text{GaAs}/\text{Al}_{0.3}\text{Ga}_{0.7}\text{As}$ MQW,

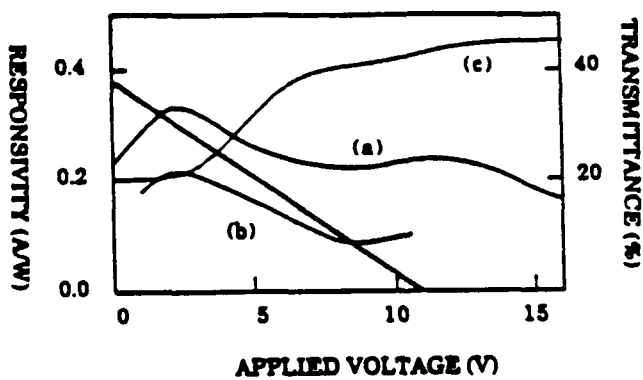
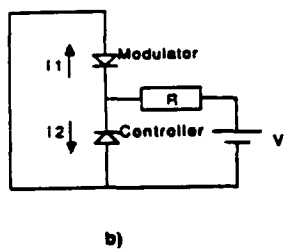
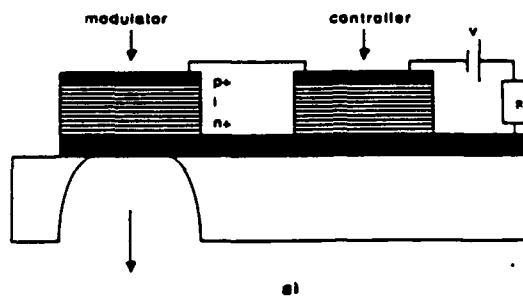
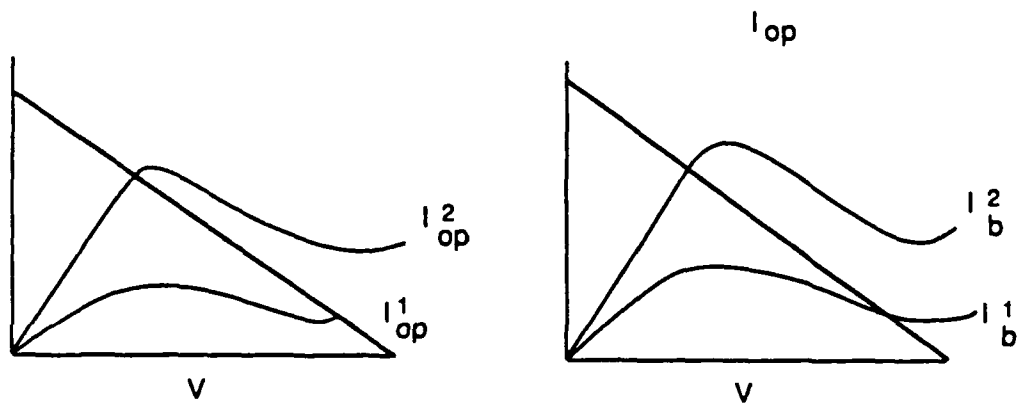
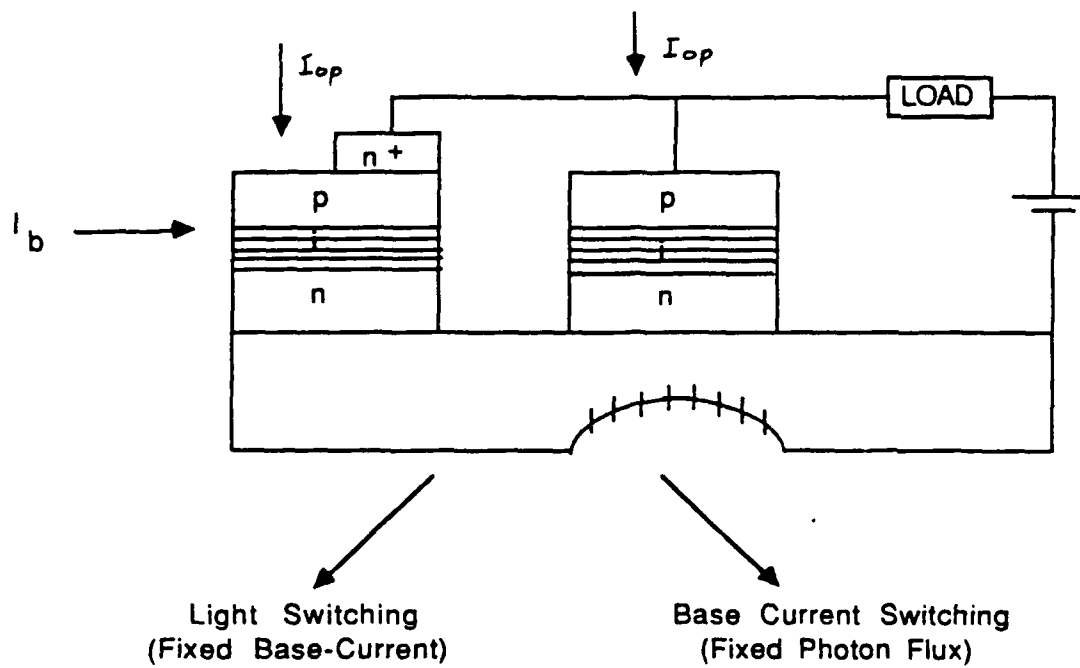


Figure 2: A schematic for the operation of the SEED. The I-V curve and the load line illustrate the switching concept.



- Integrating - Thresholding Optical Logic
- Multiple Modulator Control By One Optical Beam
- Optically Programmable Memory Cell.
- High Speed Modulation Using HBT - Microwave/Digital Technology
- Programmable Memory Cell

Figure 3: (a) A MQW-HBT structure along with schematic of the switching operation by (b) optical power and (c) base current.

which forms the essential element for the QCSE modulator and detector in the HBT. The 800 Å undoped graded layer above the MQW is to ensure that carriers emitted from the base gain sufficient energy to travel across the first few barriers of the MQW. A 150 Å thick undoped GaAs layer is included before the Be-doped base region to prevent the possible dopant out-diffusion during epitaxy. Low temperature (15 K) photoluminescence spectra of the MQW show an excitonic peak at $\lambda = 798$ nm with a full width at half maximum (FWHM) of 3 meV. The measured absorption spectrum of the MQW reveals clearly the HH and LH excitonic resonances. Device fabrication starts with the formation of emitter and collector mesas by etching in a solution of $\text{H}_3\text{PO}_4:\text{H}_2\text{O}_2$. Emitter and collector contacts are formed by electron beam evaporation of Ge/Au/Ni/Ti/Au and subsequent lift-off in acetone. The base contact is formed by deposition of Zn/Ni/Au. Both contacts are alloyed at 450° C for 60 seconds though separately, to form the respective ohmic contacts. Typical current-voltage characteristics of a HBT are shown in Fig. 4. A maximum current gain of 60 was obtained at $I_b = 17.5$ μA in a 50 μm diameter device. The high cut-in offset in V_{CE} is due to the presence of the MQW in the base-collector region. A modulator device with 50 μm diameter exhibits a very low leakage current (few pA at 8 V reverse bias). The large enhancement in the negative resistance region are quite obvious.

To measure the device operating characteristics, a tunable dye-laser and a spectrometer were used to select the optimal operating wavelength. It was found that at $\lambda = 850$ nm the photo response, both in the controller HBT and the modulator, exhibits a distinct NDR region. We briefly discuss some switching characteristics for ON/OFF optical switching. For our experiments the switching was performed between dark (OFF) and 10/ μW (ON) optical light. We found the optimal bias conditions to be $R_L = 15\text{K}\Omega$ and $V_{app} = 15\text{V}$. An 8 V swing was obtained across the controller. This is large enough to change the transmittance across a 0.6 μm thick MQW modulator by 50%. A controller output voltage corresponding to a chopped (1.5 KHz) 10 μW optical input is shown in Fig. 5. It is evident that low power photonic switching is achieved due to the gain of the phototransistor controller.

The temporal response of the device was also studied. The response time is primarily limited by the RC time constant of the bipolar transistor which is estimated to be 1 ns and the FWHM is ~ 1.5 ns. As more modulators are connected to one controller (lateral fan-out), the response speed of the system becomes slower.

1.2 Multi-Modulator Control and Amplification

As shown in the previous section, the controller device has a high built-in gain. We now examine two possible applications which utilize this gain. The first application involves the case where ON/OFF switching of the optical signal to the controller modulates the output signal through a number of modulators. For this application we operate with a wavelength which places the photon energy slightly above the exciton peak energy at zero bias, causing the negative resistance in the photocurrent. The purpose is to use the gain of the controller to control more than one modulator. Another application we explore is the case where a small increase in the optical power in the controller produces a large increase in the power out of a modulator. This "amplification" of light is also possible due to the built in gain of the controller. However, for the amplification experiments, the photon energy should be below the exciton peak so that increased photon intensity results in a lower voltage across the modulator and high

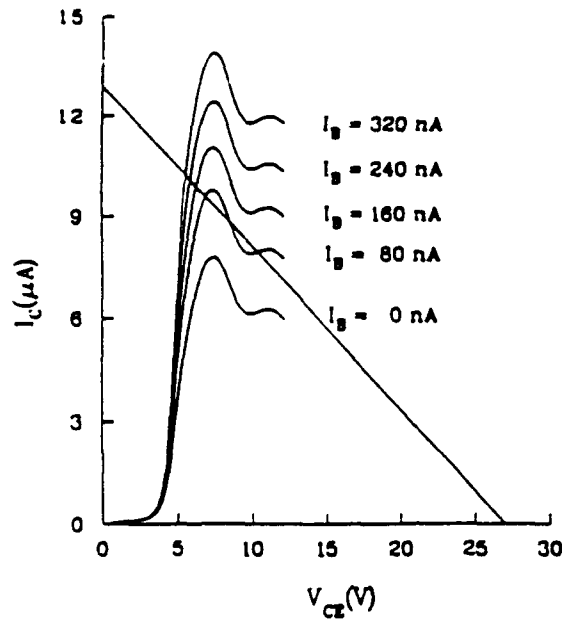


Figure 4: Measured I-V curves in a MQW-HBT.

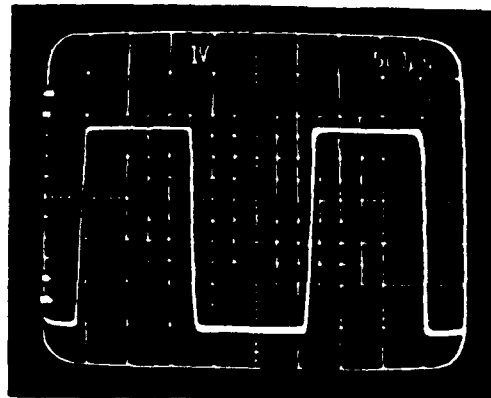


Figure 5: Switching results in a MQW-HBT. Switching is carried out by chopping an optical beam.

transmittance. The two choices for the photon energy are schematically illustrated in Fig. 1 by λ_1 and λ_2 respectively. Note that for the switching applications as the bias increases the transmittance increase, while for the amplification experiment it decrease.

In Fig. 6(a) we shown schematically the arrangement for the multi-modulator control experiment. We measure the voltage change across the modulator when the optical input (850 nm) to the controller is switched from $10 \mu\text{W}(p_i)$ to zero. The input to the modulator is maintained at a constant value of $10 \mu\text{W}$. For this switching experiment we used the parameters $V_{app} = 12 \text{ V}$ and $R = 15 \text{ k}\Omega$. The limiting factor for the number of modulators that can be attached to a controller is the photocurrent produced by the modulator. Using a modulation ratio criteria of 2:1, we need a voltage swing of 6 V to successfully control the modulators. As can be seen from Fig. 6(b), this allows us to effectively control eight modulators with a single controller.

For the use of the controller-modulator circuit for optical amplification we choose a photon energy 15 meV below the exciton peak at zero bias. The transmittance-voltage curve for this choice is shown in Fig. 7 along with the circuit configuration used. Once again we expect that the large gain of the controller will allow a small change in the controller input intensity to produce a large change in the modulator output. Figure 8 shows the modulated light P_m through the modulator as a function of incident power P_i through the controller. The results are shown for two values of the base current. As discussed in the previous section, for low-base current, the controller gain is ~ 8 , while it gains up to 35 for the base current of $4 \mu\text{A}$. As can be seen in Fig. 8 the improved gain allows a larger "amplification". Amplification values of 8 are obtained from these experiments. Both of the demonstrations in this section i.e., control of multiple modulators and optical "amplification" can find important applications in optical systems.

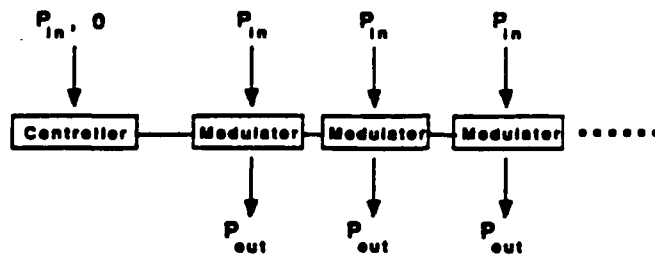
1.3 Programmable Memory Cell

When the input optical wavelength is below the HH exciton zero field energy, the I-V curves are such that a load line can have two stable points as shown in Fig. 9(a). Conditions shown as input optical power of Φ_{op}^o and I_B^o , the device has the state V_H . For storing and holding the low voltage value V_L , either the base current or the optical power can be increased so that the only stable point for the load line is a low voltage value (B on Fig. 9). Now when the hold conditions are restored the low voltage value is reached and held.

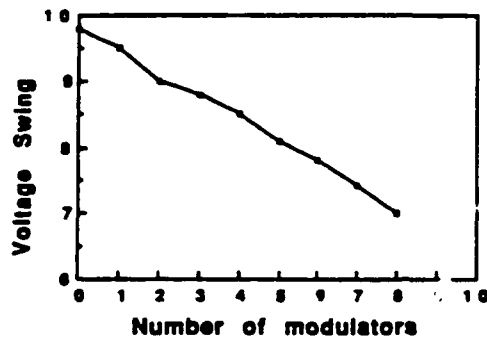
The MQW-HBT device discussed above is very well suited for the memory element because of the built in gain and consequent high noise margin⁽¹³⁾. It also has the practical aspect that the light level for all memory cells can be maintained at I_{op}^o and the memory values can be controlled through the base current. Also unlike the usual flip-flops, a single transistor is involved in the memory promising a high density level. In Fig. 10 we show some of our results for the switching and hold experiments.

1.4 Wavelength Selective Detection

An important feature of the excitonic transitions is the sharpness of the resonances. The I-V curves are thus very sensitive to the input wavelength as discussed before. If the input signal stays in a communication channel, is coming digitally and serially in

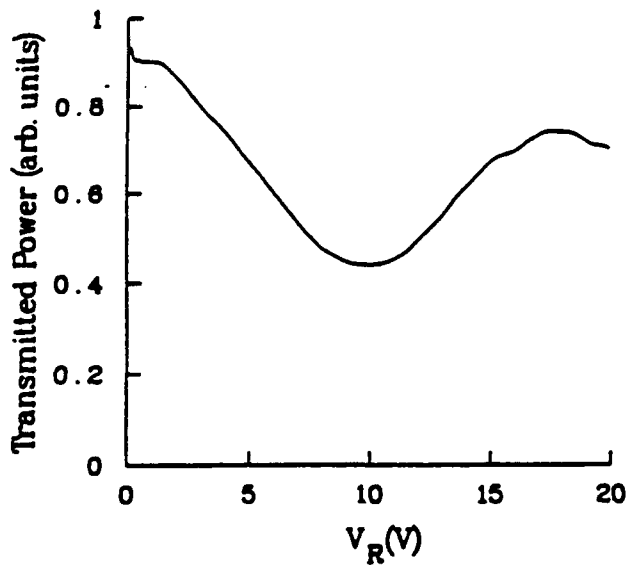


(a)

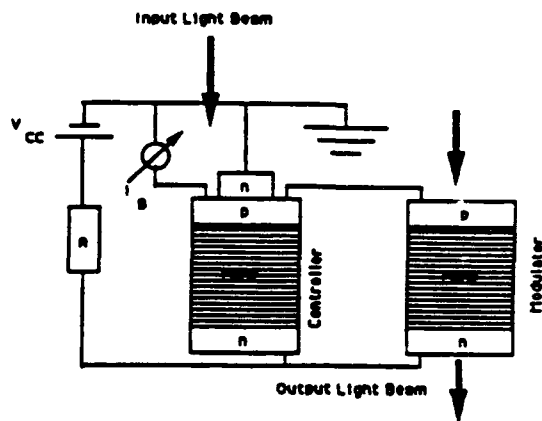


(b)

Figure 6: A schematic for the fan-out studies with results of the voltage swing obtained as a function of number of modulators.



(a)



(b)

Figure 7: (a) The transmittance-voltage curve at the photon energy used by amplification studies: (b) the circuit used in the measurements.

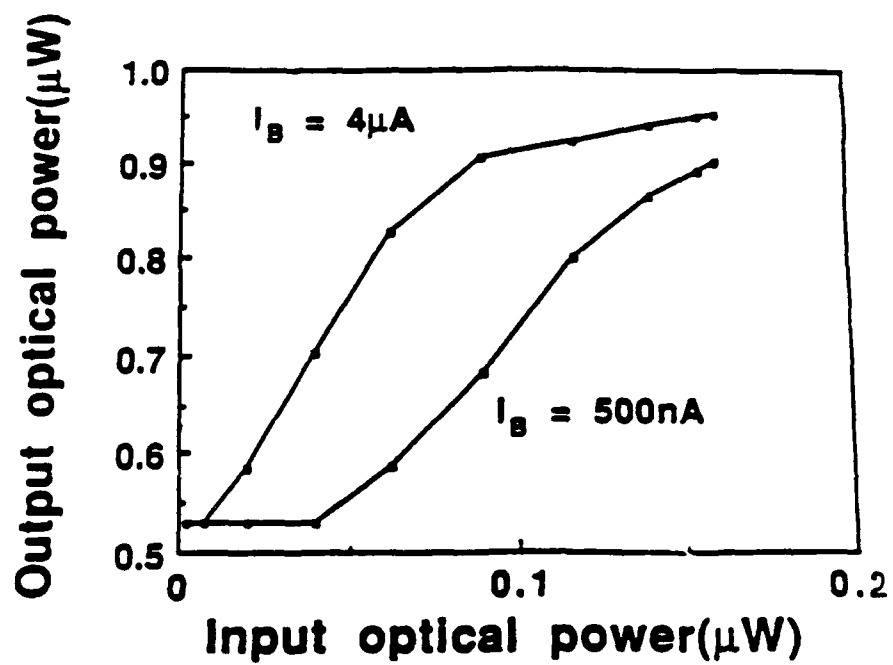


Figure 8: Measured optical amplification using the MQW-HBT.

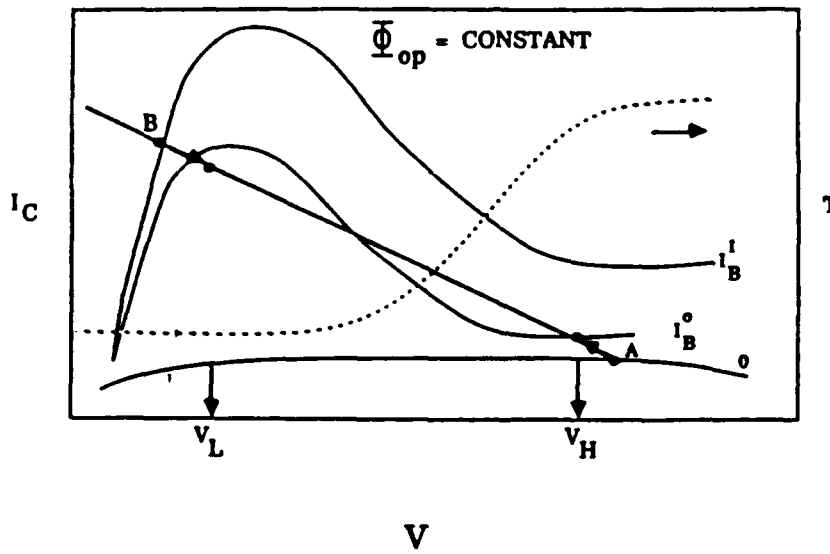
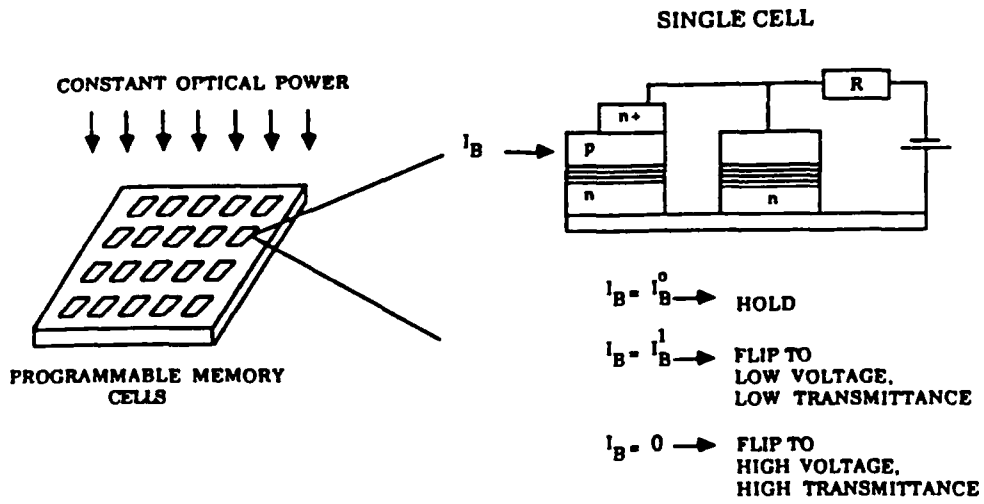


Figure 9: Schematic of the programmable memory device using the MQW-HBT. The device operation is also shown.

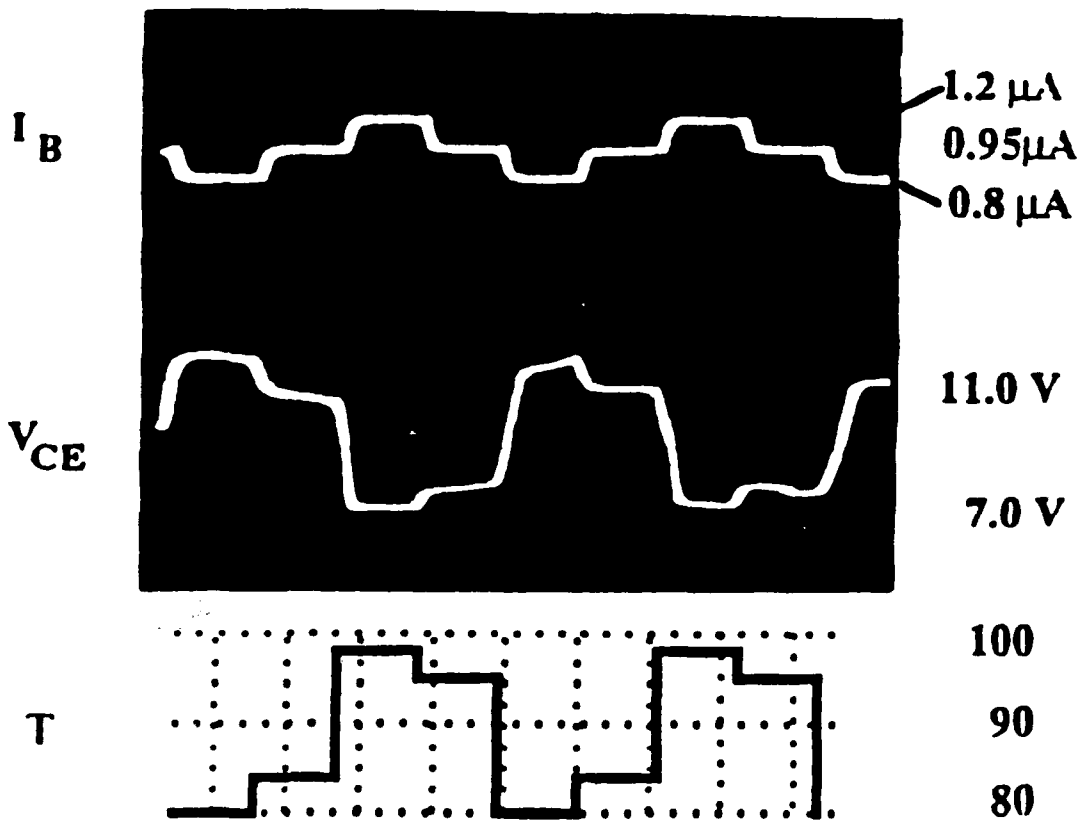


Figure 10: Measurements on switching and hold behavior of the device.

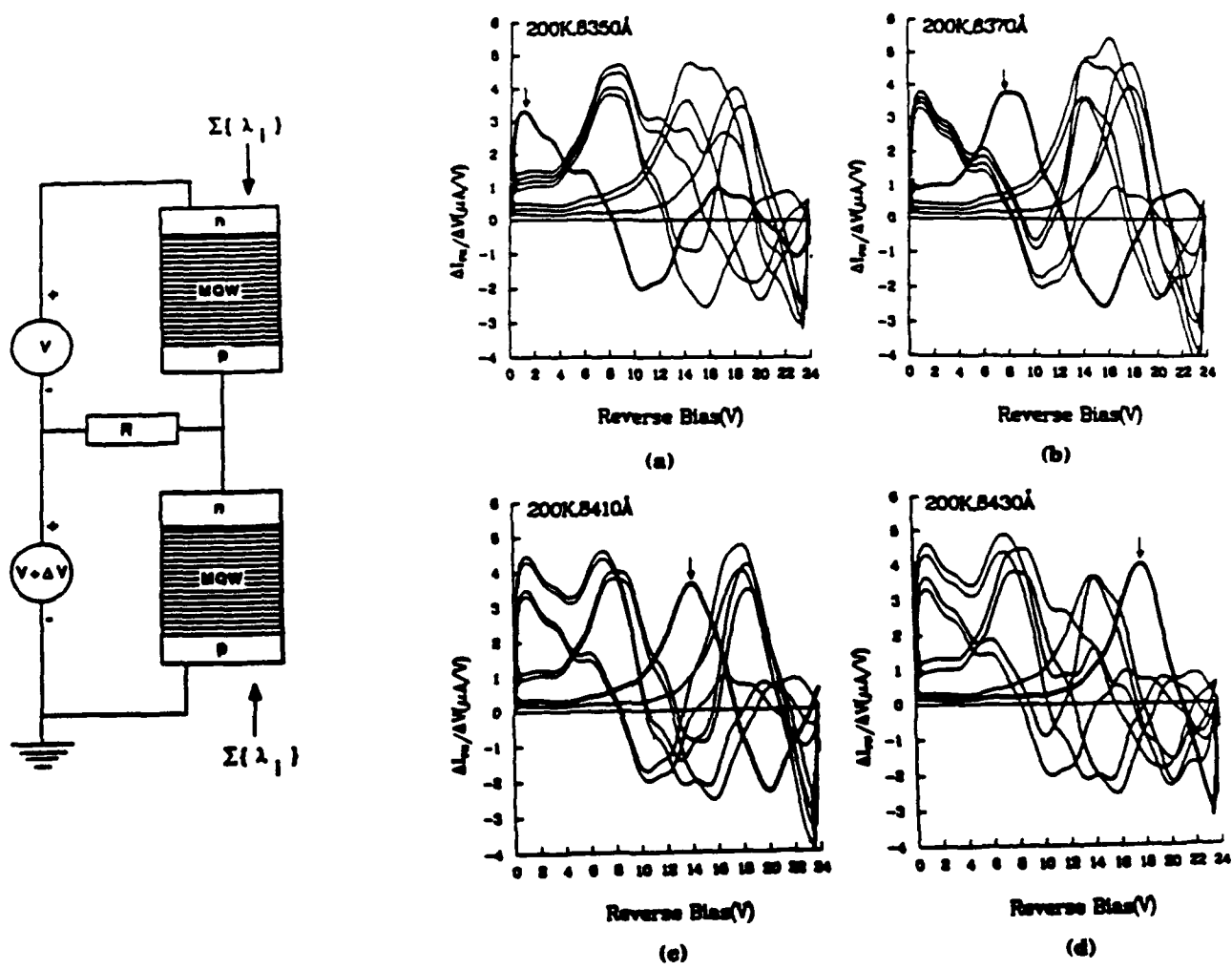


Figure 11: Schematic for the photocurrent differentiation studies circuits along with some typical results for wavelengths selective applications.

one of the several wavelengths, the excitonic detector can be tuned to either receive it or discard it. This ability is, of course quite useful, but is not as useful as the ability to do so even if several wavelength signals were coming in parallel. A simple p-i(MQW)-n diode does not have such a discrimination, but simple circuit shown in Fig. 11(a) which carries out a differentiation of the photocurrent has a strong wavelength selectivity even when a number of wavelengths are impinging in parallel. In Fig. 11(b)-11(e) we show the values of $\Delta I_{ph}/\Delta V$ at 200 K for different states of a 4-channel parallel input. The four wavelengths used are 8350Å, 8370Å, 8410Å and 8930Å. The results in bold are for the case when the ON state of only the channel b) $\lambda_i = 8350\text{Å}$; c) $\lambda_i = 8370\text{Å}$; d) 8410 and e) $\lambda_i = 8430\text{Å}$. Each of these channels can be distinguished regardless of the input of other channels if the device is biased at the points marked by the arrows in the figures. At these bias points if $\Delta I_{ph}/\Delta V$ is greater than $2\mu\text{A}/\text{V}$, the particular λ_i bit is ON (regardless of input in the other channels) and if it is less than $2\mu\text{A}/\text{V}$, it is OFF.

It has been shown that up to six channels can be selectively detected⁽¹⁴⁾. The number of channels can be further increased if the MQW structures are not made up of same size single quantum wells, but are formed from say two different size wells so as to remove the dip in absorption between the HH and LH transitions. The step function absorption profile used in the differentiation mode (Fig. 11(a)) is expected to have a very high wavelength selectivity.

5. REFERENCES

1. J. W. Goodman, *Introduction to Fourier Optics*, (McGraw-Hill, New York, 1968).
2. A. Kozma and D. L. Kelly, *Appl. Optics*, **4**, 387 (1965).
3. P. W. Smith and W. J. Tomlinson, *IEEE Spectrum*, June 1981.
4. N. Peyghambarian and H. Gibbs, *Opt. Eng.*, **24**, 68 (1985).
5. D. A. B. Miller, D. S. Chemla, T. C. Damen, A. C. Gossard, W. Wiegmann, T. H. Wood, and C. A. Burrus, *Phys. Rev. Lett.*, **53**, 2173 (1984).
6. D. A. B. Miller, D. S. Chemla, T. C. Damen, A. C. Gossard, W. Wiegmann, T. H. Wood, and C. A. Burrus, *Phys. Rev. B.*, **32**, 1093 (1985).
7. S. Hong, M. Jaffe and J. Singh, *IEEE J. Quant. Elec.*, **QE23**, 2181 (1987).
8. D. A. B. Miller, D. S. Chemla, T. C. Damen, T. H. Wood, C. A. Burrus, A. C. Gossard, and W. Wiegmann, *Opt. Lett.*, **9**, 567 (1989).
9. P. Wheatly, P. J. Bradley, M. Whitehead, G. Parry, J. E. Midwinter, P. Mistry, M. A. Pate, and J. S. Roberts, *Electron. Lett.*, **23**, 92 (1985).
10. S. Hong and J. Singh, *IEEE J. Quant. Elect.*, **25**, 301 (1989).
11. W-Q. Li, S. C. Hong, J. E. Oh, J. Singh and P. K. Bhattacharya, *Electron. Lett.*, **25**, 476 (1989).
12. S. Hong, J. Loehr, S. Goswami, P. Bhattacharya, and J. Singh, to appear in *Superlattices and Microstructures*.
13. W-Q. Li, S. Goswami, P. K. Bhattacharya, and J. Singh, to be published.
14. S. Goswami, P. Bhattacharya and J. Singh, to appear in *Superlattices and Microstructures*.

2. PUBLICATIONS AND CONFERENCE PRESENTATIONS:

1. "Implementation of Neural Network Using Quantum Well Based Excitonic Devices - Device Requirement Studies," J. Singh, S. Hong, P. K. Bhattacharya and R. Sahai, Proceedings of IEEE International Conference on Neural Networks, II, pp. II-411 (1988).
2. "System Requirements and Feasibility Studies for Optical Modulators Based on GaAs/AlGaAs Multi-Quantum Well Structures for Optical Processing," J. Singh, S. Hong, P. Bhattacharya, R. Sahai, C. Lastufka and H. Sobel, *Journal of Light-wave Technology*, **6**, p. 818 (1988).
3. "Quantum Confined Stark Effect of Excitonic Transitions in GaAs/AlGaAs MQW Structures for Implementation of Neural Networks: Basic Device Requirements," J. Singh, S. Hong, P. Bhattacharya and R. Sahai, *Applied Optics*, **27**, p. 4554 (1988).
4. "Integrated Multi-Quantum Well Controller Modulator with High Gain for Low Power Photonic Switching," W. Li, S. Hong, J. Oh, J. Singh and P. Bhattacharya, *Electronic Letters*, **25**, p. 476 (1989).
5. "Demonstration of an Integrated Multi-Quantum Well Heterojunction Bipolar Transistor with Gain for Efficient Low Power Switching," S. C. Hong, W. Li, J. Oh, P. Bhattacharya and J. Singh, *Proceedings of the Topical Conference on Quantum Wells for Optics and Optoelectronics*, March 1989, Salt Lake City.
6. "Integrated Heterojunction Bipolar Phototransistor with MQW Collector for Low Power Photonic Switching," S. C. Hong, W. Q. Li, S. Goswami, J. E. Oh, P. Bhattacharya and J. Singh, GaAs and Related Compounds Conference, p. 789 (1989).
7. "Photocurrent and Intrinsic Modulation Speeds in P-I(MQW)-N GaAs/AlGaAs Stark Effect Modulators," S. Hong, J. Loehr, S. Goswami, P. Bhattacharya and J. Singh, *Superlattices and Microstructures*, **8**, pp. 41-45 (1990).
8. "Wavelength Selective Detection Using Excitonic Resonances in GaAs/AlGaAs P-I(MQW)-N Structures," S. Goswami, P. Bhattacharya and J. Singh, *Superlattices and Microstructures*, **7**, pp. 423-426 (1990).
9. "A Programmable Memory Cell Using Quantum Confined Stark Effect in a Multi-Quantum Well Heterojunction Bipolar Transistor," W-Q. Li, S. Goswami, P. K. Bhattacharya and J. Singh, *Electronics Letters*, **27**, pp. 31-32 (1991).
10. "Wavelength Selective Detection Using Excitonic Resonances in GaAs/AlGaAs P-I(MQW)-N Structures," S. Goswami, P. Bhattacharya and J. Singh, presented at the *5th International Conference on Electro-Optic Microstructures and Microdevices*, Crete, Greece, July 31 - August 3, 1990.
11. "Implementation of Neural Networks Using Quantum Well Based Excitonic Devices - Device Requirement Studies," J. Singh, S. Hong, P. K. Bhattacharya and R. Sahai, *IEEE International Conference on Neural Networks*, San Diego, California, July 24-27, 1988.

12. "Demonstration of an Integrated Multiquantum Well Heterojunction Bipolar Transistor with Gain for Efficient Low Power Switching," S. C. Hong, W. Li, J. Oh, P. Bhattacharya and J. Singh, *Topical Conference on Quantum Wells for Optics and Optoelectronics*, March 1989, Salt Lake City.
13. "Integrated Heterojunction Bipolar Phototransistors with MQW Collector for Low Power Photonic Switching," S. C. Hong, W. Q. Li, S. Goswami, J. E. Oh, P. Bhattacharya and J. Singh, *GaAs and Related Compounds Conference*, p. 789 (1989).
14. "Novel Optoelectronic Devices for Neural Network Implementation," Invited talk at the *International Neural Network Workshop*, Jackson Hole, Wyoming, February 2-7, 1990.
15. "Integrated Multiquantum Well Heterojunction Bipolar Transistors for Optical Switching and Thresholding Applications," P. Bhattacharya, J. Singh, S. Goswami, W-Q. Li and S. C. Hong, Invited talk at the *1990 IEDM*, San Francisco, California, (1990).